Knott, T.R., et al., 2020, Discovery of two new super-eruptions from the Yellowstone hotspot track (USA): Is the Yellowstone hotspot waning?: Geology, v. 48, https://doi.org/10.1130/G47384.1

ANALYTICAL METHODS AND DATA INTERPRETATIONS

WHOLE ROCK X-RAY FLUORESCENCE (XRF) METHODOLOGY, UNIVERSITY OF LEICESTER, UK

Whole rock samples were prepared for major and trace element analysis by grinding in a Retsch planetary mill using agate pots and grinding balls. Major and trace element data were obtained on fusion beads and pressed powder pellets, respectively by X-ray fluorescence (XRF) analysis using a PANalytical Axios Advanced X-ray fluorescence spectrometer at the University of Leicester, UK (Table S2). The PANalytical Axios runs a 4Kw Rhodium anode end window ceramic technology X-ray tube. Total loss on ignition (LOI) was measured on pre-dried powders after ignition at 950°C in air for 1 hour. Instrumental conditions have been selected to avoid any significant line overlaps within the usual compositional range of most geological materials. Stability of the current generation X-Ray Spectrometry systems is such that measurements are no longer ratioed to a monitor sample to minimise instrumental drift effects but selected suitable drift monitoring samples are analysed at the commencement of each analytical run. Calibrations for major and trace element analyses were set using international rock reference material (e.g., BCR-1, BHVO-1, W-2; Table S5a-b) under the same conditions and regressing the measured count ratios against the recommended concentrations principally from Govindaraju (1994), Imai et al. (1995, 1996, 1999) and values published on the GeoREM reference site, utilising the Philips based Fundamental parameters correction technique. The analyses of international reference material indicate that precision for the observed data range and over the period of analytical work was 1 - 5% or better for major and trace elements (Tables S2a and S2b).

ELECTRON MICROPROBE METHODOLOGY, OPEN UNIVERSITY, MILTON KEYNES, UK

Thin sections (30 microns) were cut from select samples of each member of the Cassia Formation, and these were subsequently polished and carbon-coated prior to electron microprobe analysis.

Analyses of pyroxene phenocrysts (Table S3) were obtained at the Open University, Milton Keynes using a Cameca SX100 electron microprobe. An operating voltage of 20 kV and probe current of 20 nA (measured on a Faraday cage) with a 10 micron beam diameter were used for quantitative analysis. Data were reduced using the PAP correction routine of Pouchou & Pichoir (1985).

PALAEOMAGNETIC METHODOLOGY UNIVERSITY OF CALIFORNIA, SANTA CRUZ, USA

Laboratory work was conducted at the University of California, Santa Cruz, USA. Magnetic remanence measurement and automated progressive AF demagnetization up to 200 mT was performed on a 2G cryogenic magnetometer and Sapphire Instruments demagnetizer using a customized sample handler and software (Morris et al., 2009). The order of axes used during progressive 3-axis static alternating field demagnetization was permuted as described by Finn and Coe (2016). Thermal demagnetization was carried out in a custom built oven housed in a magnetically shielded room along with the AF demagnetizer and cryogenic magnetometer. Fisher statistics (Fisher, 1953) and principal component analysis (Kirschvink, 1980) were used to average individual sample directions and to calculate the best fit lines to demagnetization data, respectively.

Where tilt corrections were required to minimise the effects of post-emplacement tectonic rotations, a best-fit correction was applied where multiple eruption-units were sampled at a single site within stratigraphic continuity (e.g., both the Grey's Landing and McMullen Creek ignimbrites together). No tilt corrections are used at site locations where only the Grey's Landing Ignimbrite was observed, which at all locations had negligible dips (<5°), and these were used as reference sites during correction (e.g., within Rogerson graben, see supplementary Table S4). The only exception is the "Gwin Springs" site where only the Grey's Landing ignimbrite is exposed; here the apparent effects of post-emplacement tilting were minimised using measured dip and strike data at the site (see Table S4). The best-fit horizontal rotations were chosen to simultaneously improve the cluster tightness of both the Grey's Landing and McMullen Creek site mean directions by using the same strike and dip for both units at each location. The cluster tightness can be described by the precision parameter (k) associated with the mean of the group of site direction. The cluster tightness of the two groups is improved by minimizing the sum of 1/k for both groups. The underlying assumption here is that both tuff units experienced the same post emplacement horizontal axis rotation (tilting) for each location where they are stratigraphically adjacent. The estimated best-fit corrections generally fit strike and dips measured in the field (see Table S4). We preferred this best fit method over using the measured strike and dips wherever possible due to the possibility of initial deposition onto a slope, and uncertainties in the field measurements. This offered a notable improvement to the correlation strength, eliminating erroneous scatter due to tilting and issues with correction using measured attitudes..

CA-ID-TIMS U-PB METHODODOLOGY, BRITISH GEOLOGICAL SURVEY, UK

CA-ID-TIMS U-Pb analyses were carried out at the NERC Isotope Geosciences Laboratory, British Geological Survey, UK. Following analytical and data reduction methods described by Tapster et al. (2016) and utilising the ET535 EARTHTIME mixed tracer (Condon et al. 2015).

The correction for initial ^{230}Th disequilibrium within the zircon was conducted using an assumed Th/U melt value of 4.36 ± 0.44 1σ for sample RG001 (Grey's Landing Ignimbrite) and 4.28 ± 0.44 1σ for sample RC-10.1-005 (McMullen Creek ignimbrite) derived from the whole rock Th/U variation for the crystal poor eruptive units. The mean Th/U for > 20 SRP eruption-units between ca. 11-8 Ma is 4.53 ± 0.50. In the instances where a correction for initial common Pb (PbC) from inclusions that were not leached during chemical abrasion is applied, we derived a PbC model isotopic composition at ~9 Ma from the mean and SD of 7 whole rock values for the equivalent crystal poor volcanic sequences from Wright et al. (2002). These values are provided in supplementary Table S6.

Date uncertainties are described as analytical uncertainty only to allow direct comparison between samples. In order to compare dates with other U-Pb data that is not traceable to the EARTHTIME tracers an additional ~3 kyrs uncertainty must be added, and an additional ~20 kys uncertainty must be added to compare with data from other isotopic systems such as the Ar-Ar system. All uncertainties are at 2σ level unless otherwise stated.

Results and interpretations:

Grey's Landing Ignimbrite (basal vitrophyre; Sample RG001)

25 single crystal $^{206}Pb/^{238}U$ dates range from ca. 8.6 – 9.6 Ma, with one substantially older date at ca. 10.6 Ma (Table S5). Dispersion within the population is well in excess of that expected for a single population (MSWD = 320, n=24) indicating that there is a significant component of crystal recycling (antecrystic zircon).

The total mass of U within post-CA zircon fractions ranged from 115 – 4520 pg with a 377 pg U median. Zircon < ca. 9.3 Ma typically contained < 300 pg total U yielding $^{206}Pb/^{204}Pb$ 30-157 and single ^{230}Th corrected data point 2σ precision of 50-400 kyrs, with the exception of one analysis which contained an order of magnitude greater U (4.5 ng) and yielded single data point 2σ precision of 11 kyrs. Notably this poses a challenge for statistical age interpretation that uses any form of precision-based weighting. Therefore, we must consider the scenarios whereby (1) this single high-U, high precision date represents the timing of crystal growth at the time of eruption, or (2) the date represents an antecryst and therefore offers a maximum constraint on the timing of eruption.

Total PbC ranges from 0.30-4.0 pg with a median of 0.68 pg that is in excess of the ~0.5 pg total procedural blank over the analytical period. Thus we also consider the impact on the age interpretations of different scenarios where all PbC is attributed to laboratory blank and where laboratory blanks of PbC = 0.3 ± 0.1 pg, 0.5 ± 0.2 pg and 0.7 ± 0.4 pg are fixed. In the latter scenarios, any remaining PbC is attributed to a component of common Pb (equating in composition to the PbC model (Table S6) derived from WR Pb isotope date given in Wright et al., (2002) contained as inclusions within the zircon that were not leached away during chemical abrasion.

We interpret ages from 1) the youngest single fraction date (although this is not a robust reproducible age interpretation); 2) a weighted mean date including the youngest 5 analyses that form a statistically acceptable MSWD excluding the date of the youngest high-U crystal; 3) a weighted mean date of all youngest crystals excluding the date of the high-U crystal that form a statistically acceptable MSWD;

and 4) the youngest statistically acceptable MSWD of a population that includes the youngest high-U crystal (see Table S7).

The compilation of interpreted weighted mean $^{206}Pb/^{238}U$ dates that excludes the youngest high-U fraction, ranges between 8.668 ± 0.058 Ma (n=5, MSWD 1.4) and 8.772 ± 0.085 Ma (n=6, MSWD 1.5) and are in broad agreement with the youngest single dates 8.57 ± 0.13 Ma to 8.60 ± 0.17 Ma. The youngest weighted mean date that includes the young high-u fraction varies only by a few kyrs and reaches a maximum 8.865 ± 0.011 (n=7, MSWD = 1), with the rejection of 3 younger singles dates where a correction for initial PbC is applied (Table S7). We suggest this captures the maximum possible date for eruption from the data, but is unlikely to capture latest autocrystic crystal growth.

On the basis that the youngest high-U most precise date may reflect an antecrystic date, as supported by the necessity to reject younger dates from the weighted mean calculation that includes this fraction in some permutations of initial PbC, the preferred age of eruption is selected as **8.716 ± 0.065 Ma** (n=6, MSWD=1.8, 0.5 ± 0.2 pg PbC attributed to laboratory blank). Probability density plots show clusters of antecrytic dates around 9.0-9.2 Ma, also showing a peak at ca. 9.35 Ma (Fig. S1).

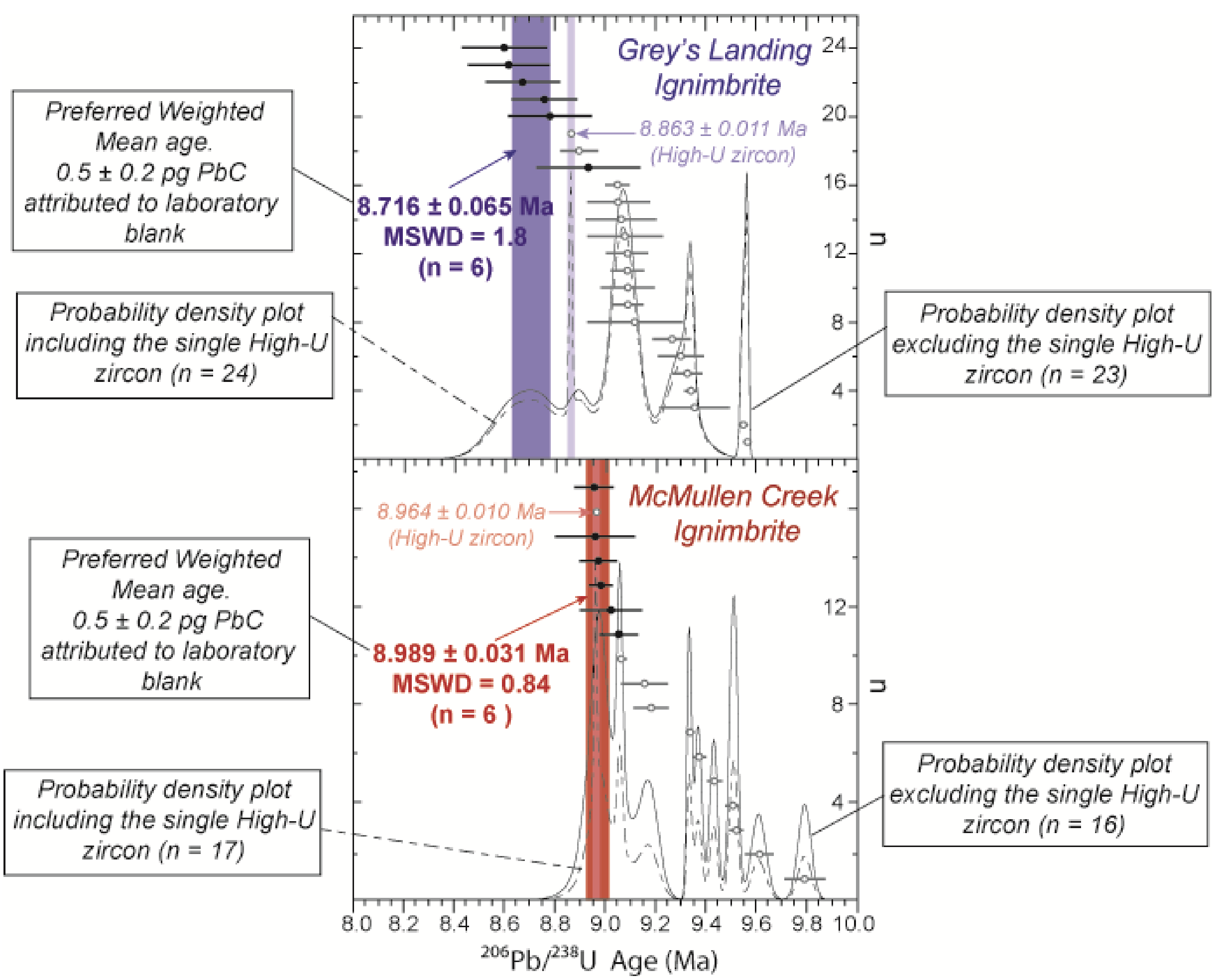

Fig. S1. Zircon $^{206}Pb/^{238}U$ single crystal age determinations and probability density of the two super-eruptions with 2σ uncertainty. Filled (black) symbols indicate zircons used in preferred weighted mean age interpretations (age in bold); open circles are potential antecrysts, including a single high-U zircon age.

McMullen Creek Ignimbrite (basal vitrophyre; Sample RC-10.1-005)

17 single crystal $^{206}Pb/^{238}U$ dates range from ca. 8.9 – 9.8 Ma (Table S5). Dispersion in excess of a single population is evident (MSWD 190, n=17). Indicating there is significant component of antecrystic zircon. The total mass of U in each fraction varies by over an order of magnitude (190-5000 pg U) with a median of 742 pg U.   As with RG001, the youngest high-U analysis poses a problem for statistical analysis using weighting of data as it is significantly more precise and therefore receives the greatest weighting (>90%) yet it may represent an antecrystic growth, or simply lie outside of the 2SD range due to analytical scatter. We examine age interpretations from the youngest statistically acceptable weighted means that both include, and exclude, this fraction, in addition to eruption interpretations based on the youngest (non-reproducible) single date.

Total PbC varies to excess of the total procedural blank over the analytical period, between 0.4 to 1.9 pg, thus we again consider the impact of different amounts of initial PbC on the age interpretation over scenarios as described for RG001.

Interpreted weighted mean $^{206}Pb/^{238}U$ dates excluding the youngest, high-U fraction, range from 8.956 ± 0.027 Ma (n=5, MSWD =0.89) to 9.000 ± 0.034 Ma (n=6, MSWD =0.75). These correspond well with the weighted mean $^{206}Pb/^{238}U$ dates that include the high-U fraction, 8.9651 ± 0.0090 Ma (n=7, MSWD =1.7) to 8.9668 ±0.0094 Ma (n=7, MSWD =1.3) and the youngest single $^{206}Pb/^{238}U$ dates, 8.954 ± 0.078 Ma to 8.9642 ± 0.009 Ma. This indicates that the date of the youngest high-U fraction cannot be differentiated from other approximations of eruption and give confidence to the interpretation that the age of this unit is ca. 8.95-9.00 Ma.

Our preferred, conservative eruption age estimate is **8.989 ± 0.031 Ma** (n=6, MSWD=0.84, 0.5 ± 0.2 pg PbC attributed to laboratory blank). However it should be noted that the most precise high-U single date, that is not included within the age interpretation, lies at the younger end of the 2σ uncertainty range (see Fig. S1). Probability density plots illustrate clusters of antecrytic dates at ca. 9.1-9.2 Ma, and ca. 9.35-9.6 Ma (Fig. S1).

Repose time between the McMullen Creek and Grey's Landing eruptions

The overlying nature of the two volcanic units provides an a priori knowledge of the relative age of these units. Whilst there are multiple age interpretations of both units we can constrain the permitted repose periods between these units. Repose times between the weighted mean interpretations that exclude the high-U most precise young data points, vary between 228 ± 90 kyrs to 303 ± 60 kyrs and is therefore within uncertainty of the estimated repose times that range between 356 ± 187 kyrs and 384 ± 152 kyrs calculated from single youngest date age interpretations (see Table S7). This indicates a likely repose time on the order of ca. 200-300 kyrs between units. The minimum repose times between eruptions that is feasible from the data is captured by the temporal difference between the date interpretations of RC10.5 and the weighted mean date of RG001 that includes the high-U fraction, which is typically older than the youngest statistically acceptable weighted mean of the sample (Table S7). These differences cluster between ca. 90 to 140 kyrs and always result in resolvable differences between units.

REFERENCES (*INCLUDING THOSE IN SUPPLEMENTARY TABLES*)

Andrews, G.D.M., Branney, M.J., Bonnichsen, B., and McCurry, M., 2008, Rhyolite ignimbrites in the Rogerson graben, southern Snake River Plain volcanic province: Volcanic stratigraphy, eruption history and basin evolution: Bulletin of Volcanology, v. 70, p. 269–291, doi: 10.1007/s00445-007-0139-0.

Bonnichsen, B., 1982a, Rhyolite lava flows in the Bruneau-Jarbidge eruptive center, southwestern Idaho, Cenozoic geology of Idaho. Idaho Bureau of Mines Geology Bulletin, v. 26, p. 283–320.

Bonnichsen, B., Christiansen, R.L., Morgan, L.A., Moye, F.J., Hackett, W.R., Leeman, W.P., Honjo, N., Jenks, M.D., Godchaux, M.M., 1989, Excursion 4A: Silicic volcanic rocks in the Snake River Plain-Yellowstone Plateau province. In: Chapin, C.E., Zidek, J. (eds). Field excursions to volcanic terranes in the western United States; Volume II, Cascades and Intermountain West. NM Bur. Mines. Mineral. Resourc. Mem. v. 47, p. 135–182.

Bonnichsen, B., Leeman, W.P., Honjo, N., McIntosh, W.C., Godchaux, M.M., 2008, Miocene silicic volcanism in southwestern Idaho: geochronology, geochemistry, and evolution of the central Snake River Plain. Bull. Volcanol. v. 70, p. 315–342.

Condon, D. J., B. Schoene, N. M. McLean, S. A. Bowring, and R. R. Parrish., 2015, Metrology and Traceability of U-Pb Isotope Dilution Geochronology (EARTHTIME Tracer Calibration Part I). Geochimica et Cosmochimica Acta, v. 164, p. 464-480.

Finn, D. R., & Coe, R. S., 2016, A new protocol for three□axis static alternating field demagnetization of rocks. Geochemistry, Geophysics, Geosystems, v. 17(5), p. 1815-1822.

Fisher, R.A., 1953, Dispersion on a sphere: Royal Society of London Proceedings, v. 217, p. 295–305.

Govindaraju, K.,1994, 1994 compilation of working values and sample description for 383 geostandards: Geostandards Newsletter, v. 18, p. 1–158.

Hackett, W.R., Moye, F.J., Bonnichsen, B., 1989, Day 5 Silicic volcanism in the SRP-YP province. New Mex. Bur. Mines Min. Res. Mem. v. 47, p. 160–167.

Honjo, N., McElwee, K.R., Duncan, R.A., Leeman, W.P. (1986). K-Ar ages of volcanic rocks from the Magic Reservoir eruptive center, Snake River Plain, Idaho. Isochron/West, v. 46, p. 15–17.

Imai, N., Terashim,a S., Itoh, S., and Ando, A., 1995, 1994 compilation of analytical data for minor and trace elements in seventeen GSJ geochemical reference samples, "Igneous rock series": Geostandards Newsletter, v. 19, p. 135–213.

Imai, N., Terashima, S., Itoh, S., and Ando, A., 1996, 1996 compilation of analytical data on nine GSJ geochemical reference samples, "Sedimentary rock series": Geostandards Newsletter, v. 20, p. 165–216.

Imai, N., Terashima, S., Itoh, S., and Ando, A., 1999, 1998 compilation of analytical data for five GSL geochemical reference samples, the "Instrumental analysis series": Geostandards Newsletter, v. 23, p. 223–250.

Kirschvink, J.L., 1980, The least-squares line and plane and the analysis of paleomagnetic data: Geophysical Journal of the Royal Astronomical Society, v. 62, p. 699–718.

Knott, T. R., M. J. Branney, M. K. Reichow, D. R. Finn, R. S. Coe, M. Storey, D. Barford, and M. McCurry, 2016a, Mid-Miocene record of large-scale Snake River-type explosive volcanism and associated subsidence on the Yellowstone hotspot track: The Cassia Formation of Idaho, USA, Geological Society of America Bulletin, doi:10.1130/B31324.1.

Knott, T. R., M. K. Reichow, M. J. Branney, D. R. Finn, R. S. Coe, M. Storey, and B. Bonnichsen, 2016b, Rheomorphic ignimbrites of the Rogerson Formation, central Snake River Plain, USA: Record of mid-Miocene rhyolitic explosive eruptions and associated crustal subsidence along the Yellowstone hotspot track, Bulletin of Volcanology, v. 78(4), p. 1–25.

Konstantinou, A., Strickland, A., Miller, E. L., and Wooden, J. P., 2012, Multistage Cenozoic extension of the Albion–Raft River–Grouse Creek metamorphic core complex: Geochronologic and stratigraphic constraints: Geosphere, v. 8, no. 6, p. 1429–1466. doi: 10.1130/GES00778.1.

Michalek, M., 2009, Geological Map of parts of the Lake Hills and Carey Quadrangles, Blaine County, Idaho. M.S. Thesis, Idaho State University, USA. 1:12,000.

Morris, E.R., Schillinger, W., Coe, R.S., Pluhar, C.J., and Jarboe, N.A., 2009, Automating the 2G superconducting rock magnetometer for single-solenoid alternating field demagnetization: Geochemistry. Geophysics. Geosystems, v. 10.

Oakley, W.L., Link, P.K., 2006, Geologic map of the Davis Mountain Quadrangle, Gooding and Camas Counties, Idaho. Idaho Geological Survey. 1:24,000. Idaho Geol. Surv. Geologic Map 49.

Pouchou, J.L., and Pichoir, F., 1985, “PAP” procedure for improved quantitative analysis: Microbeam. Analysis, v. 20, p. 104–105.

Smith, C.L., 1966, Geology of eastern Mount Bennett Hills, Camas, Gooding, and Lincoln counties, Idaho: University of Idaho Ph.D. dissertation. 129 pp.

Tapster, S., Condon, D.J., Naden, J., Noble, S.R., Petterson, M.G., Roberts, N.M.W., Saunders, A.D. & Smith, D.J., 2016. Rapid thermal rejuvenation of high-crystallinity magma linked to porphyry copper deposit formation; evidence from the Koloula Porphyry Prospect, Solomon Islands. Earth and Planetary Science Letters, v. 442, p. 206-217.

Wright, K.E., McCurry, M., Hughes, S.S., 2002, Petrology and geochemistry of the Miocene tuff of McMullen Creek, central Snake River Plain. In: Bonnichsen, B., McCurry, M., White, C.M. (eds). Tectonic and magmatic evolution of the Snake River Plain volcanic province. Idaho Geol. Surv. Bull. v. 30, p. 177–194.